Aerosol Science and Technology, 38(S1):215–228, 2004

ISSN: 0278-6826 print / 1521-7388 online
DOI: 10.1080/02786820390229525

A Method for the In Situ Measurement of Fine Aerosol Water Content of Ambient Aerosols: The Dry-Ambient Aerosol Size Spectrometer (DAASS)

Charles O. Stanier, Andrey Y. Khlystov, Wanyu R. Chan, Mulia Mandiro, and Spyros N. Pandis
Department of Chemical Engineering, Carnegie Mellon University, Pittsburgh, Pennsylvania

Hygroscopic growth of atmospheric particles affects a number of environmentally important aerosol properties. Due to the hysteresis exhibited by the aerosol hygroscopic growth, the physical state of particles and the amount of aerosol water are uncertain within a wide range of relative humidities (RHs) found in the troposphere, leading to uncertainties in optical and chemical properties of the aerosol. Here we report the design and tests of an automated system that was built to assess the amount of aerosol water at atmospheric conditions. The system consists of two scanning mobility particle sizers (SMPS) and an aerodynamic particle sizer (APS) that measure the aerosol size distribution between 3 nm and 10 μm in diameter. The inlets of the instruments and their sheath air lines are equipped with computer-controlled valves that direct air through Nafion dryers or bypass them. The Nafion dryers dehydrate the air streams to below 30% RH at which point ambient particles are expected to lose most or all water. The switch between the dried and the ambient conditions occurs every 7 min and is synchronized with the scan times of the aerosol spectrometers. In this way the system measures alternatively dried (below 30% RH) and ambient aerosol size distributions. A comparison of the ambient RH and the dried RH size distributions and the corresponding integrated volume concentrations provides a measure of the physical state of particles and the amount of aerosol water. The aerosol water content can be treated as a growth factor or as an absolute quantity and can be calculated as a time series or as a function of RH (humidigram). When combined with aerosol composition measurements, the DAASS can be used to compare hygroscopic growth models and measurements.

Received 23 October 2002; accepted 22 April 2003.

This research was conducted as part of the Pittsburgh Air Quality Study, which was supported by the US Environmental Protection Agency under contract R82806101 and the US Department of Energy National Energy Technology Laboratory under contract DE-FC26-01NT41017.

Address correspondence to Spyros Pandis, Department of Chemical Engineering, Carnegie Mellon University, 5000 Forbes Ave., Pittsburgh, PA 15213, USA. E-mail: spyros@andrew.cmu.edu

INTRODUCTION

The absorption of water by atmospheric aerosols with increasing relative humidity (RH) influences their size, composition, lifetime, chemical reactivity, and light scattering. Water is the most prevalent aerosol component at RHs above 80% and is often a significant component at lower RHs (Hanel 1976). Accordingly, hygroscopic growth is important in a number of air pollution problems, including visibility impairment, climate effects of aerosols, acid deposition, long-range transport, and the ability of particles to penetrate into the human respiratory system.

A number of laboratory investigations of water uptake by model or smog chamber aerosols have been conducted. Laboratory studies have used single-particle levitation (Tang and Munkelwitz 1993; Chan 1992; Wagner et al. 1996) and hygroscopic tandem DMA (H-TDMA) (Rader and McMurry 1986) to investigate water uptake, deliquescence, and crystalliation of a number of inorganic compounds. More recently, these techniques have been used to investigate hygroscopicity in organic compounds and organic–inorganic mixtures (Xiong et al. 1998; Virkulla et al. 1999; Cruz and Pandis 2000; Peng et al. 2001; Cocker et al. 2001a, b; Brooks et al. 2002).

Most field studies of water uptake in ambient aerosols have used a H-TDMA (McMurry and Stolzenberg 1989; Berg et al. 1998; Dick et al. 2000). Results of H-TDMA studies are reviewed by Cocker et al. (2001c) and typically classify particles into more hygroscopic and less hygroscopic fractions, with the number of fractions, relative size of fractions, and growth factors varying at different sites. Other techniques devised to measure water uptake include RH-conditioned nephelometry (Rood 1987; ten Brink et al. 2000; Day et al. 2000), filter analysis by gravimetry (Vartiainen et al. 1994), filter analysis by chemical analysis (Ohta et al. 1998), filter analysis by beta attenuation (Speer et al. 1997), observation by Fourier transform infrared spectroscopy (Han and Martin 1999; Onasch et al. 1999; Martin et al. 2001; Han et al. 2002), and in situ measurement of

evaporated water (Lee and Hsu 1998). Kreisberg et al. (2001) used an optical particle counter for in situ automated measurement of dried, humidified, and ambient size distributions.

Several thermodynamic models have been developed that calculate the water uptake of pure and mixed salts (see Ansari and Pandis 1999 and references therein). Recently, these methods have been extended to particles containing organic compounds (Saxena and Hildemann 1997; Ansari and Pandis 2000; Clegg et al. 2001; Ming and Russell 2002).

While this body of experimental, theoretical, and field research has significantly advanced the understanding of water uptake by aerosols, significant uncertainties remain. First, there is a limited amount of information about the liquid water content of "real" particles in the atmosphere. Second, many aerosol compositions exhibit hysteresis in aerosol water content, potentially existing at more than one thermodynamically stable state. Third, field data are required to validate and improve models for mixed organic–inorganic–water models. Finally, a method is needed for direct in situ measurement of this important particulate matter component. Therefore, there is a need for additional field measurements that focus on the in situ aerosol water content, crystallization behavior, comparison with mass-based measurements, and the influence of organic compounds.

This work describes a new field instrument, the dry-ambient aerosol size spectrometer (DAASS), for the in situ measurement of the atmospheric fine aerosol liquid water content. The DAASS was designed and deployed during the Pittsburgh Air Quality Study (PAQS), and its design, calibration, data reduction procedure, and first results are reported in this work.

EXPERIMENTAL

The DAASS is an automated combination of aerosol-sizing instruments that measures the dried (<30%) and ambient RH aerosol number distribution. The aerosol water content is calculated from the difference of the dried and ambient volume distributions.

The design goals for the DAASS included:

- Measurement of the dried (<30% RH) aerosol size distribution from 3 nm–10 μm microns for several months with a frequency of at least 4 times per hour.
- Measurement of the ambient aerosol water content up to ambient RH levels of 90% RH and on a frequency of at least once per hour.
- Automatic operation and data acquisition with minimal maintenance for field deployment.
- Operation from -15°C to 35°C temperatures, and dewpoints up to 25°C.

The DAASS includes three particle-sizing instruments with associated supporting equipment, as shown in Figure 1. The particle-sizing instruments include two scanning mobility particle sizers (SMPS) and one aerosol particle sizer (APS). The SMPS instruments size particles from 3–80 nm (TSI 3936N25) and 13–680 nm (TSI 3936L10), while the APS (TSI 3320) sizes particles from 0.5–10 μm. These systems are referred to as the Nano-SMPS, SMPS, and APS systems in this article. Two separate RH controlled inlets served the aerosol-sizing instruments. One inlet conditioned aerosols for the SMPS systems, while a separate inlet conditioned aerosols for the APS. Supporting these components are a dry air supply system and humidity-conditioning systems for the sheath air flows of both SMPS systems and the APS.

All components were housed in a weatherproof plywood enclosure with a volume of 3.6 m^3. To meet the goal of measuring the ambient aerosol size distribution at ambient temperature and RH without active temperature and RH control, the instruments, particularly the differential mobility analyzer (DMA) columns, needed be kept at ambient temperature. In the first set of tests, all equipment, including the DMA columns, was placed inside the enclosure, and temperatures were kept near ambient using a large exhaust fan ($\sim$35 m^3 min^{-1}). In spite of the large flow of outside air, the DMA column temperatures were elevated about 4°C relative to ambient and were therefore drying the ambient samples. The ambient scans reached only approximately 80% of the ambient RH (e.g., outdoor RH of 95% yielded an ambient channel RH of around 76%). To keep the DMA column temperatures closer to ambient, the columns were moved to a protected ledge just outside the enclosure while fans pulled ambient air over them. This configuration improved performance, and the DMAs then achieved greater than 90% of ambient RH (e.g., outdoor RH of 95% yielded an ambient channel RH of greater than 86%). The effects of this mismatch are discussed in the data reduction section below.

During winter, the enclosure was maintained at a minimum temperature of 9°C, which was required for the maintenance of condenser and saturator temperature setpoints in the Condensation Particle Counters (CPCs). This did not significantly affect the final sheath and aerosol relative humidities because the DMA columns were outside the enclosure at (or close to) the outdoor temperature. However, the aerosol flow did pass through this heated enclosure, and the charger was located in the enclosed section of the inlet. This caused the minimum RH encountered by the aerosol flow and the RH (and therefore size) during charging to be different from the final RH at the DMA column. In future deployments of the DAASS, it is recommended that the entire inlet be placed outside of the enclosure in a shaded, ventilated area. The effects of this RH minimum are considered below in the data-reduction section.

Drying of aerosol streams was accomplished using Nafion membrane dryers (Permapure MD-110, Toms River, NJ, USA). Single-tube dryers with stainless steel housings were selected for drying aerosols rather than multitube dryers to limit losses (Woo et al. 2001). For ambient RH measurements, the dryer could be bypassed using automated valves. For the SMPS system, three-way solenoid valves (Alcon U33-43-21-12, Itasca, IL, USA) were used. For the APS inlet, flow selection between the dried and ambient inlet was achieved using full-bore ball

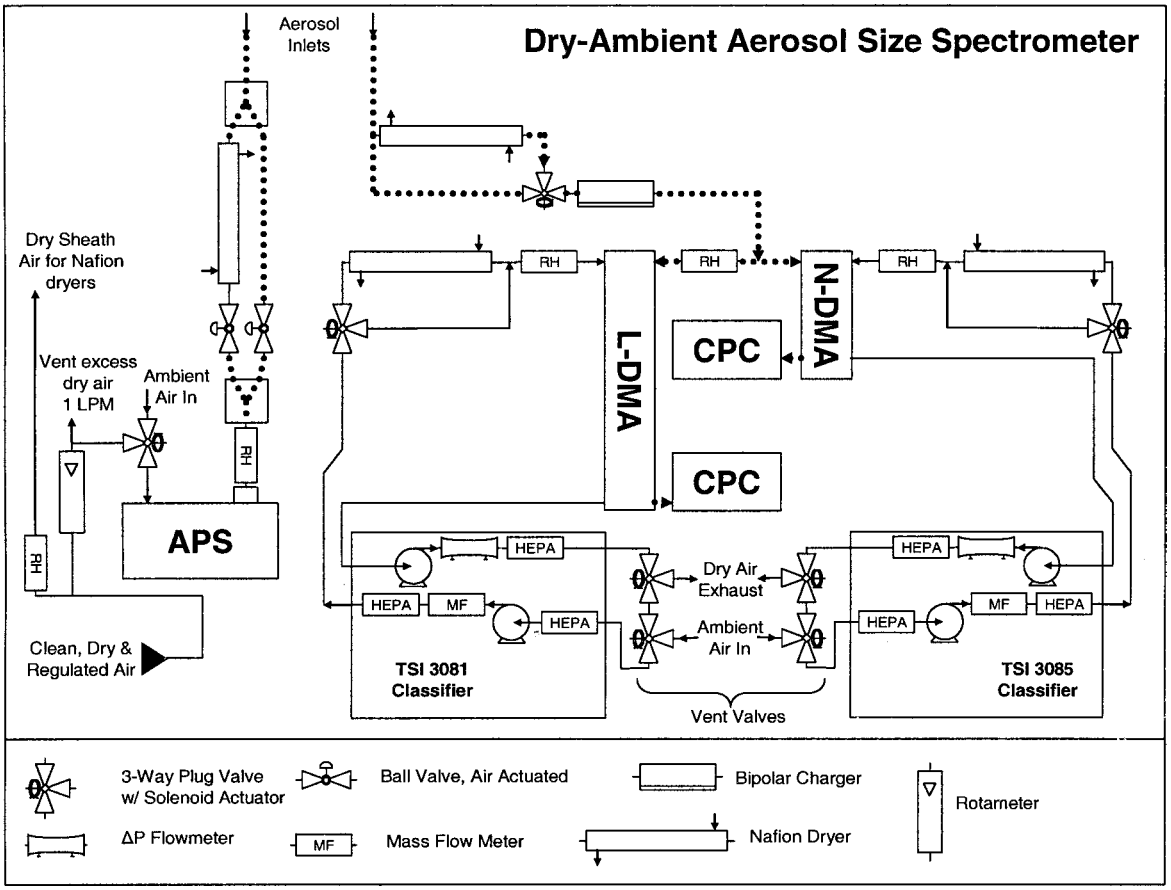

Figure 1. Flow diagram of DAASS. Aerosol streams are shown by dotted lines and other flows are indicated by solid lines.

valves (Swagelock SS-41S2-31DDM) with orifice diameters that matched tubing inner diameters. Copper and stainless steel tubing was used throughout to minimize particle losses.

The APS was modified slightly to allow for drying. With factory settings, the APS samples 5 liters per minute (LPM) and then separates the flow into a 1 LPM aerosol flow and a 4 LPM sheath flow. The sheath flow is filtered and returned in the time-of-flight section of the instrument. In the DAASS system, the dry-ambient inlet sampled 1 LPM and was connected directly to the APS inner nozzle. Particle-free air was supplied at atmospheric pressure directly to the APS sheath air inlet (Figure 1). Depending on the sampling mode, this air was at ambient RH or dried. The standard APS pump and flow control was used for both the aerosol and sheath flows.

In the SMPS systems, the aerosol is assumed to equilibrate with the sheath flow RH because of the 0.3–6 s exposure time of aerosols to the sheath flow (this assumption is considered in the data-reduction section). In the data analysis, it is the SMPS sheath flow RH that is used to analyze particle size as a function of RH. However, in the APS, the aerosol has a much shorter exposure time to the sheath air ($<10^{-4}$ s). In that case, the aerosol is assumed to be equilibrated at the aerosol stream RH and unaffected by the sheath RH.

Operation of the dry-ambient SMPS systems required three flow configurations of DMA sheath air: dried, ambient, and vent. The flow configurations for these modes are shown in Figure 2. In dried and ambient modes, the sheath air ran in a closed loop and passed through dryers or bypassed them, depending on the mode. After the dried scans, the system was put in "vent" mode and the sheath flow was switched to a once-through flow configuration. Dry air was exhausted from the system and ambient RH air was drawn into the system.

Drying of sheath air flows for the SMPS systems was accomplished using Nafion membrane dryers (Permapure PD-50T and PD-200T). Multitube dryers were selected to accommodate the flowrates, which were 3.2 and 7.0 LPM. These dryers were rated to achieve dewpoints of -15°C for incoming air at a 20°C dewpoint using shell-side utility air supplied at a -40°C dewpoint. This system achieved RHs in sheath air of less than 15% during the initial summer tests. However, during the winter tests, silica gel desiccant was added to assist in the drying. The winter drop in performance of the membrane dryers was partly due to problems in supplying -40°C dew point utility air during winter, and partly due to the need to reach lower dewpoints in winter than in summer to achieve RHs below 30% at ambient temperatures. During the coldest periods of the study (-10°C), DMA

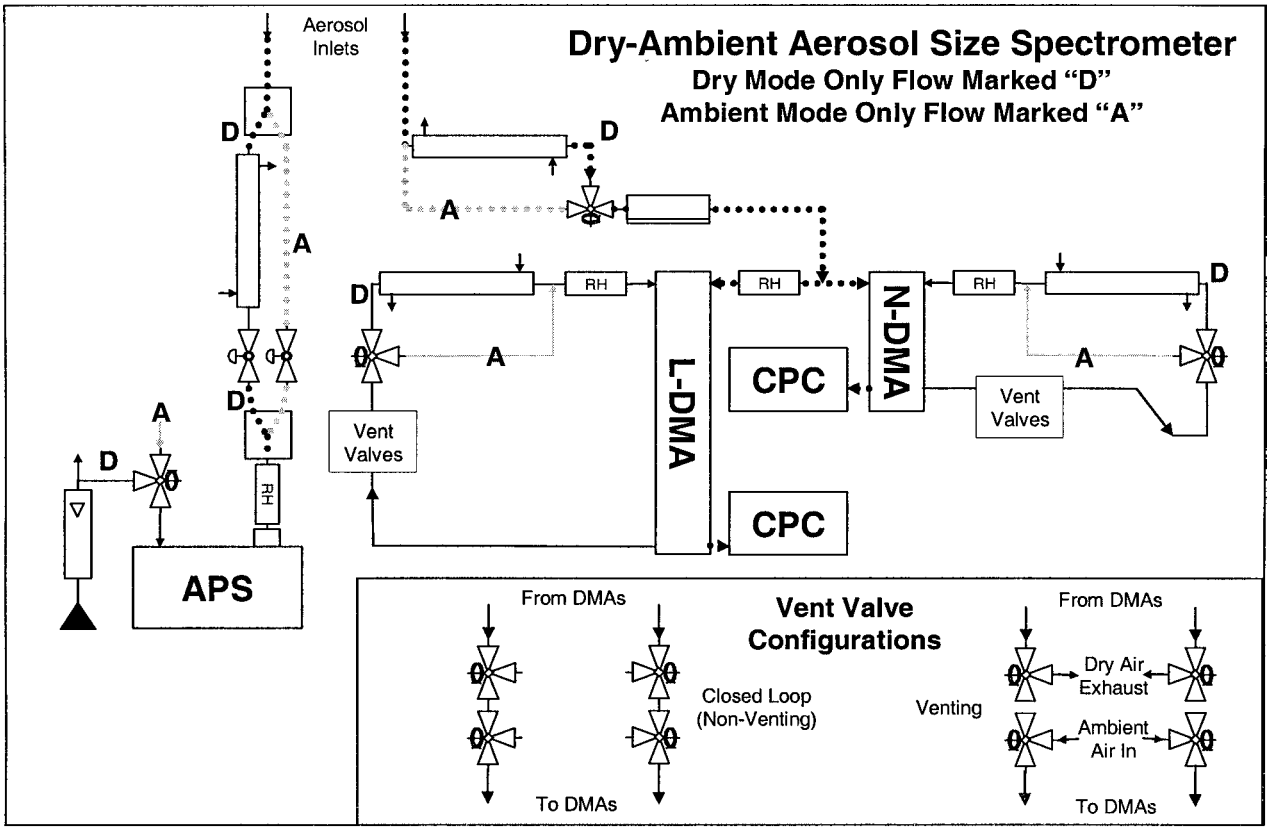

Figure 2. Dry, ambient, and vent configurations of the DAASS System. Dark flow paths labeled with "D" are only active during the dried mode. Light-colored flow paths labeled with "A" are only active in the ambient sampling mode. The third flow configuration is the venting of air from the sheath loops, shown in the lower righthand inset.

sheath air dewpoints of less than −32°C were required. Figures 3 and 4 show examples of the RH cycling achieved in the field for the SMPS systems and the APS, respectively. Two ambient cycles and two dry cycles are shown. The SMPS sheath air responded quickly when the drying cycle started. The venting took longer, and the RH decreased somewhat during the ambient RH scans.

This slight mismatch in outdoor and SMPS ambient channel sheath flow RHs (evident in Figure 3) occurred during the duration of the PAQS. The mismatch was caused by insufficient purging of dry air from the system during the vent mode, which was limited by the strength of the standard sheath and bypass blowers in the TSI 3080 DMA. In future DAASS deployments, it is recommended that a supplemental vacuum be used to assist in purging the system during the vent stage. Other explanations, such as a leak at the three-way solenoid for the dryer bypass, and a positive pressure leak from the sheath- to the tube-side of the dryers, were ruled out. When the vent time was increased from 5 min to 8 min for a test in August 2001, the outdoor-ambient water content mismatch decreased.

Raw particle count data from SMPS systems, temperatures, and RHs were acquired using a PC that also controlled solenoid valves responsible for selecting the operation mode (ambient, dried, or vent). Figure 5 shows an example of dried and wet size distributions measured during 1 h. During that hour, the DAASS measured four dried size distributions at around 14% RH and 4 size distributions at 64% RH.

CALIBRATION AND TESTING

A number of characterization tests were performed in the laboratory. Goals during the calibration and characterization stage included inlet loss characterization, absolute sizing accuracy, sizing precision between ambient and dried inlet paths, and sizing precision when two instruments measured particles of the same size.

The APS time-of-flight response was calibrated using monodisperse aerosols prior to deployment in the field. This was done using PSL spheres (Duke Scientific, Palo Alto, CA, USA) at diameters equal to 600 nm, and 2.1 μm and with monodisperse ammonium sulfate aerosols with aerodynamic diameters from 0.5 to 1.6 μm. Above 2.1 μm, the factory time-of-flight calibration curve was used.

After the APS calibration, all three instruments of the DAASS system were checked for sizing accuracy simultaneously with monodisperse aerosols fed through a common inlet. PSL spheres

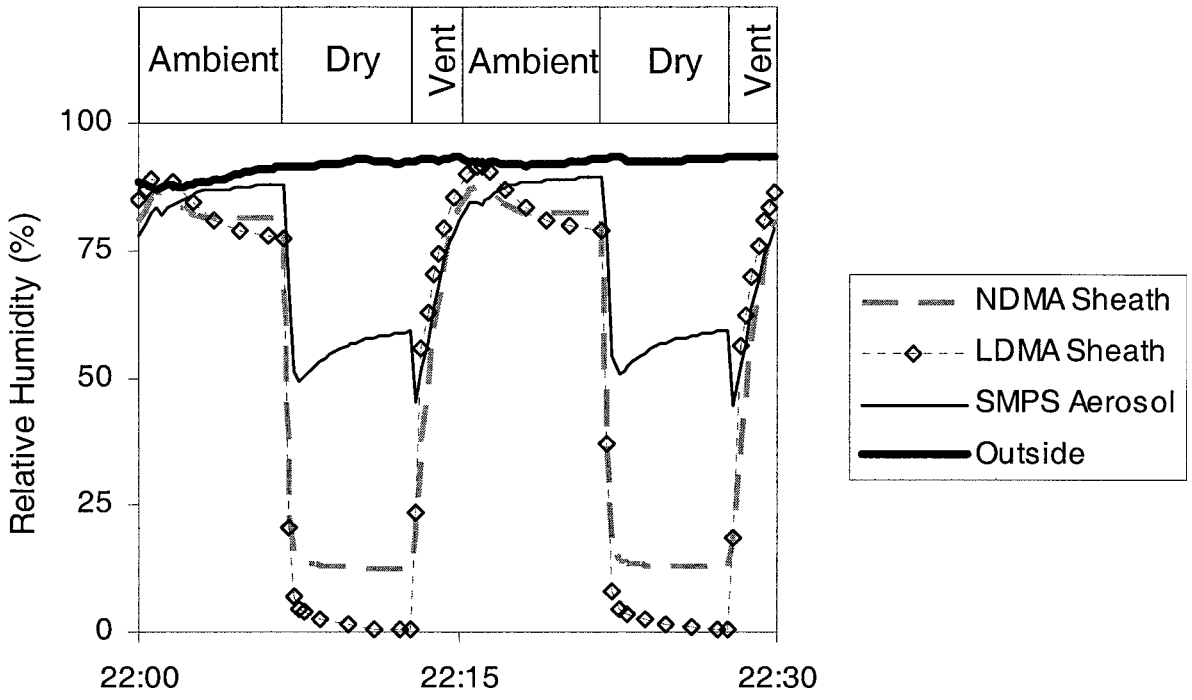

Figure 3. Example of RH time series in the SMPS instruments in DAASS. The SMPS Aerosol RH is the air sample RH before it enters the SMPS and is exposed to the sheath RH and further dried.

(Duke Scientific, Palo Alto, CA, USA) at diameters equal to 150 nm, 500 nm, 600 nm, and 2.1 μm were used.

The nano-SMPS system and SMPS system measurements overlapped in the diameter range from 13–80 nm. The SMPS and APS systems overlapped from 542–680 nm (mobility equivalent size). Sizing precision between dried and ambient inlets, and sizing from instrument to instrument in overlapping size ranges, were checked by sizing monodisperse ammonium sulfate through a common inlet to the DAASS in 14 different size ranges from 20–900 nm. Differences in particle sizing between instruments and between ambient and drying inlet channels were less than 3% across the entire size range. Size-dependent inlet losses for the SMPS inlet were determined by measuring the difference in total particle counts across the DAASS inlet (including

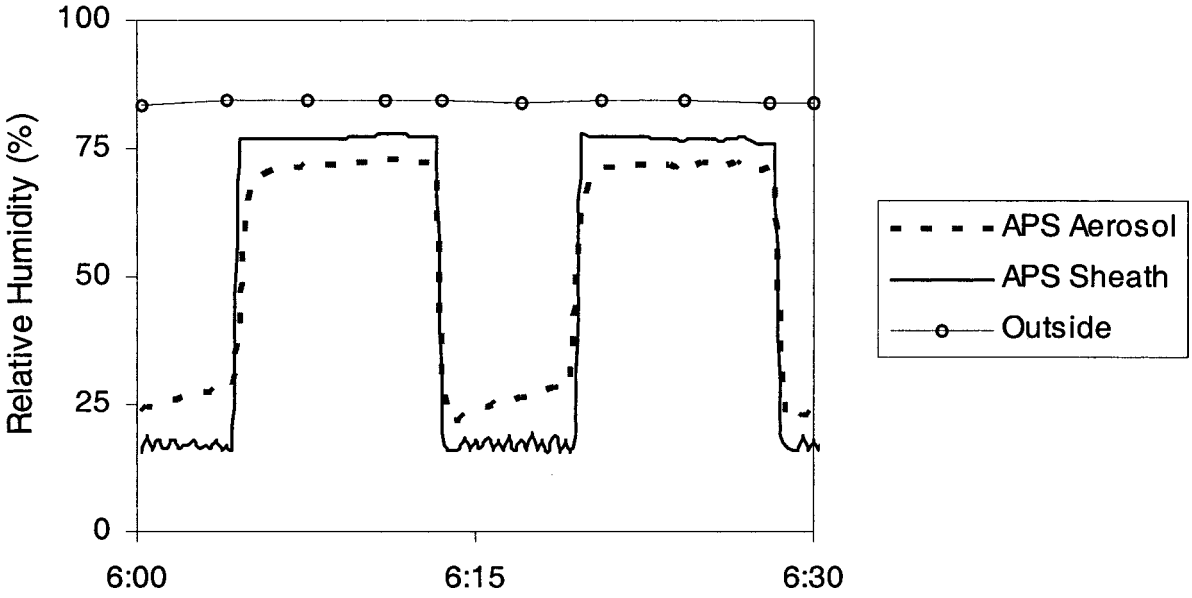

Figure 4. Example of RH time series for APS portion of DAASS.

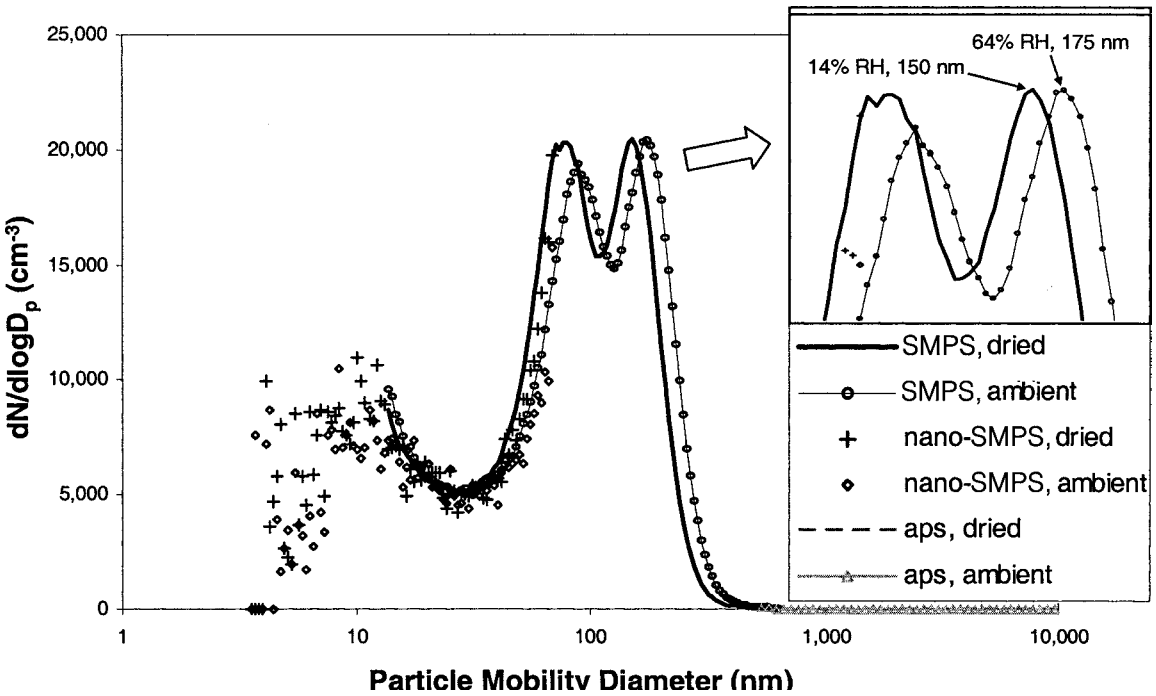

Figure 5. Dried and ambient number size distributions measured during the PAQS. Shown are one hour averages for 22:00–23:00 EST on 3 July 2001. Each of the distributions is the average of 4 ambient and 4 dried distributions.

the aerosol dryer, dryer bypass line, neutralizers, and aerosol RH probe). Particle losses below 20 nm were estimated using empirical particle loss correlations from Willeke and Baron (1993). Default manufacture-counting efficiencies were used for the CPC 3010 and CPC 3025.

The APS RH-conditioning inlet was designed for maximum possible particle transmission by minimization of tubing restrictions and bends. An inlet transmission efficiency was calculated accounting for turbulent inertial impaction to the inlet tubing walls with enhanced depositions at restrictions and bends (Willeke and Baron 1993). The calculated transmission was nearly 100% for 0.5 μm particles and greater than 90% through 2.5 μm, but it fell off to 85% transmission at 5 μm.

APS counting efficiencies from Leinert and Weidensohler (2000) were used in data reduction and ranged from 58% for 512 nm, to 90% at 1 μm, to 100% at 1.33 μm. The APS 3320 is known to suffer from false counts, or "ghost particles" in sizing channels greater than 2.5 μm due to recirculation of small particles (Armendariz and Leith 2002). This behavior could clearly be seen in the APS 3320 data, and the reported size distributions, especially the surface area and volume distributions, are elevated, sometimes significantly, above 2.5 microns.

After all of these basic system characterizations were performed, the DAASS was used to measure diameters of hydrated and dried ammonium sulfate particles. This test was performed at the PAQS central sampling site by filling a 2 m^3 teflon bag with polydisperse ammonium sulfate particles. The ammonium sulfate was drawn from the Teflon bag, through a humidifier, and into the DAASS system which sampled alternately at the elevated (hydrated) RH and a lower RH (<10% sheath RH). The results of the test are shown in Figure 6, and they show reasonable agreement with calculated ammonium sulfate growth data (Ansari and Pandis 1999).

DATA REDUCTION: CALCULATION OF WATER CONTENT FROM AEROSOL SIZE DISTRIBUTIONS

Merging of Separate Size Distributions into One Size Distribution

The raw SMPS size distributions were inverted by the TSI SMPS program (Version 3.2), and the APS distributions were inverted by the TSI Aerosol Instrument Manager program (Version 4.3). These inverted size distributions were then further corrected for counting efficiencies and inlet losses using the approach outlined in the previous section. The three different instrument distributions (nano-SMPS, SMPS, and APS) were merged to form a single size distribution for each 7.5 min sampling interval. Merging size distributions between the nano-SMPS and SMPS instruments in the overlapping region of 13–80 nm was accomplished by using nano-SMPS data up to 30 nm and then SMPS data above 30 nm. This creates a potential discontinuity in the merged size distribution at 30 nm. During most periods of operation, the agreement between the nano-SMPS and SMPS in the overlap region was within 10%. However, when the strength of local sources varied rapidly relative to the 5 min

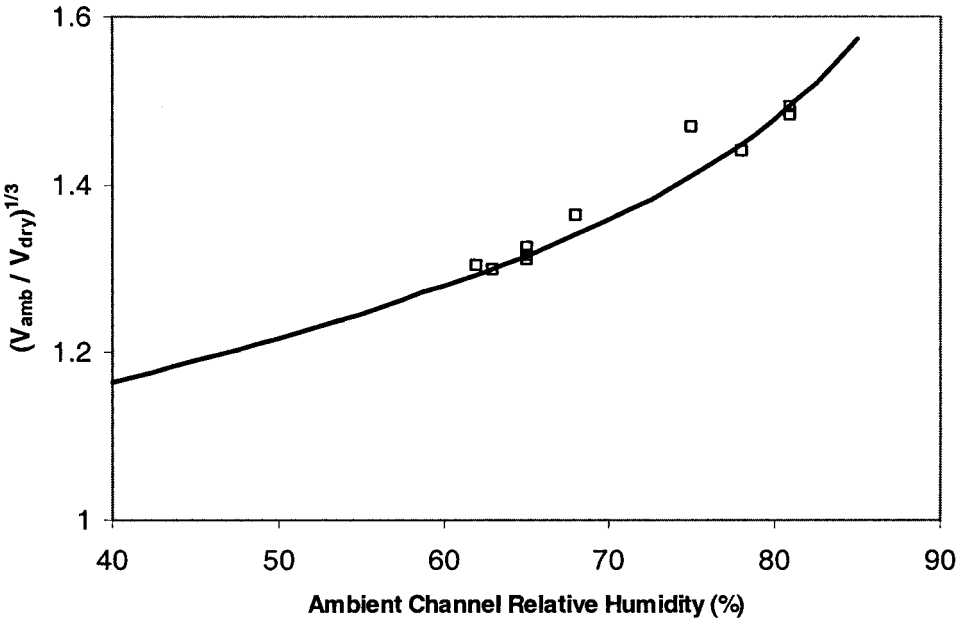

Figure 6. Theoretical (line) and measured (squares) growth factors for ammonium sulfate aerosol. Data for diameter growth factors calculated from Ansari and Pandis (1999). V_{amb} and V_{dry} are the aerosol volumes measured by the DAASS system in the ambient and dried configurations.

scan time, the agreement between the two instruments was not good on a distribution-by-distribution comparison. During periods of highly variable particle size distributions, 1 h averaging reduced but did not always eliminate the discontinuity in the size distribution at 30 nm. This limits the use of the data taken during these periods for applications that depend on the shape of the number distribution between 20 and 40 nm. However, for applications using the aerosol volume distribution, the discontinuity is not a serious issue.

Merging the SMPS and APS data was more involved due to the inherent difference between the electrical mobility measured by the SMPS and the aerodynamic diameter measured by the APS. The procedure used is explained in detail in Khlystov et al. (2004a). Briefly, an apparent density was selected to minimize the difference between the SMPS and APS number distributions in the overlap region. Thus, the shape of the APS distribution was preserved, while the x axis of the APS-measured size distribution was shifted to achieve a good fit with the SMPS-measured size distribution.

Calculation of Aerosol Water Content

A number of related calculations can be performed with the size distributions measured by the DAASS. The selection among the data reduction methods depends on the application. Described below are calculations for (1) volume growth factors, (2) $PM_{2.5}$ water content, (3) efflorescence branch humidigrams, and (4) mass growth factors. The first two calculations focus on measuring aerosol water at ambient RH. The third examines water content as a function of RH, and the last is necessary for comparison of DAASS data to mass-based aerosol water correlations and models. The first three calculations are performed with data solely from the DAASS, while the fourth calculation requires aerosol composition data.

As discussed in the experimental section, the ambient channel RH was slightly lower than the outdoor RH. Therefore, for the calculations presented below, it should be recognized that they are calculated and reported as a function of the ambient channel RH rather than the outdoor RH.

Calculation of Volume Growth Factor. Once the size distributions are merged, hygroscopic growth factors are calculated for pairs of ambient and dried size distributions using the volume distributions and assuming a single, size-independent growth factor GF_{VOL}:

$$GF_{VOL} = \frac{V_{RH2}}{V_{RH1}} = \frac{\int_0^{D_{RH2}} D^3 n^o_{N,RH2}(\log D) d\log D}{\int_0^{D_{RH1}} D^3 n^o_{N,RH1}(\log D) d\log D}, \quad [1]$$

where D is the particle diameter, V_{RH2} and V_{RH1} are the aerosol volume concentrations measured using the ambient (RH2) and dried (RH1) inlets, $n^o_{N,RH2}$ and $n^o_{N,RH1}$ are the ambient and dried aerosol size distributions, and D_{RH2} and D_{RH1} are appropriately selected limits of integration. Figure 7 shows an example of the relationship between hypothetical dried and ambient size distributions (assuming a single size-independent growth factor) and the limits of integration. For this study, focusing on the water content of the fine aerosol, an upper integration limit D_{RH2} of 2.5 μm was used. This limit is analogous to the size selection performed by the $PM_{2.5}$ cyclone often employed in

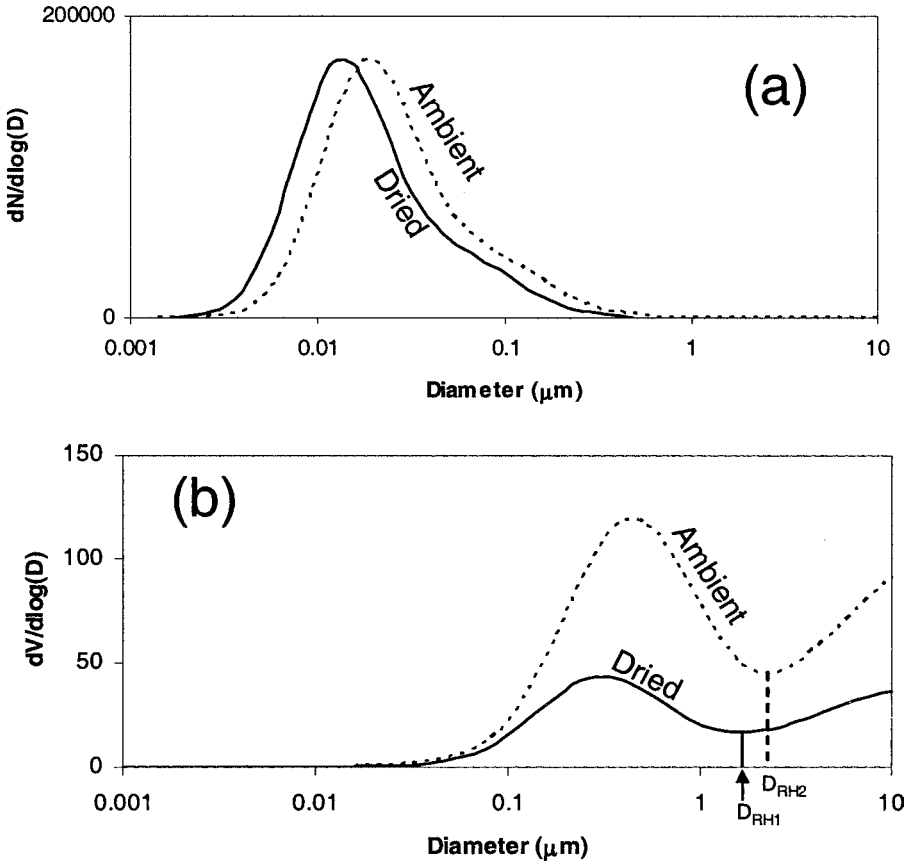

Figure 7. Illustration of the difference between dried and hydrated number and volume distributions. The figure shows a hypothetical trimodal log-normal distribution being shifted by a size-independent growth factor. The volume growth factor calculated in this study is the ratio of the volume integrals. The shifting of the upper volume integration limit with hygroscopic growth (Equation (2)) is shown by the difference between D_{RH2} and D_{RH1}.

aerosol sampling. Using larger diameters was not possible due to the ghost particle artifact in the APS 3320 volume distributions (Armendariz and Leith 2002). The lower limit of integration is theoretically zero, but any value where there is minimal aerosol volume smaller than that size is acceptable. The integration limits for the dried and ambient size distributions are related by the volume (or diameter) growth factor, again assuming a single, size-independent growth factor:

$$D_{RH2} = D_{RH1}\sqrt[3]{GF_{VOL}} \quad [2]$$

Equations (1) and (2) can be solved iteratively, given any pair of size distributions to find a volume growth factor GF_{VOL} that accounts for the differences between the ambient and dried volume distributions.

A brief discussion of the assumption of a single growth factor is instructive, as several H-TDMA investigations (Cocker et al. 2001b and sources therein) have shown that urban aerosols are usually externally mixed, with two or more populations of aerosols with different hygroscopicities. What is calculated by Equations (1) and (2) is approximately the volume-weighted average growth factor of the various externally mixed aerosol subpopulations. Interpretation of this growth factor (as a volume-weighted average) is relatively straightforward unless the limit of integration D_{RH2} is inappropriately selected and a significant fraction of the particle volume lies above the limit. Simulations with log-normal externally mixed aerosol modes of different hygroscopicities show that the growth factor calculated by Equations (1) and (2) may be biased low under this circumstance. This error is expected to be small for the PAQS when an upper integration limit of 2.5 μm is used, as most aerosol volume is less than 2.5 μm, and coarse aerosols are expected to be less hygroscopic than the accumulation mode.

As the dried and ambient aerosol distributions are not measured at the same time but are separated by some sampling interval Δt, steady increases or decreases in the aerosol volume will lead to biases in the growth factor calculated by Equation (1). This can be corrected for with the following correction factor β:

$$GF'_{VOL} = GF_{VOL}\beta = GF_{VOL}\frac{1}{1 + \frac{V'_{dry}}{V_{dry}}\Delta t} \quad [3]$$

where Δt is the amount of time by which the dried measurements precede the ambient measurements and V'_{dry} is the rate of change of the dry aerosol volume with respect to time. In the limits where the dried and ambient measurements are performed simultaneously or the dry aerosol volume is stable with respect to time, the correction factor β goes to unity. This factor was usually between 0.97 and 1.03 for the PAQS.

As the DAASS method relies on the difference between two aerosol size distributions measured at different times (about 7 min from the start of the ambient scan to the dried scan), variability in the underlying aerosol size distribution on a timescale of shorter than a few minutes can lead to random error in water-content calculations. Variability in the mean and average rate of change of the dried volume for each hour is calculated and propagated through the water content calculations as uncertainty in the parameters $\mathrm{GF_{VOL}}$ calculated in Equation (1) and β calculated in Equation (2). Calculated growth factors for four days of sampling are shown in Figure 8. The time series shows that growth factors are not a simple function of RH and that they can change rapidly with changing meteorology and composition.

Calculation of $PM_{2.5}$ Water Content at Ambient Channel RH. Using the growth factor calculated above in Equation (1), the aerosol water content can be estimated. The method uses only data from the DAASS and relies on two assumptions: (1) water is the only semivolative species causing a volume change; and (2) volume additivity between aerosol water and nonvolatile aerosol components. Applying these assumptions, we can write Equation (4),

$$V_{\mathrm{H2O,RH2-RH1}} \cong V_{\mathrm{RH2}} - V_{\mathrm{RH1}}, \qquad [4]$$

where $V_{\mathrm{H2O,RH2-RH1}}$ is the volume of evaporated water from the ambient (RH2) channel to the dried (RH1) channel. Combining Equations (1) and (4),

$$V_{\mathrm{H2O,RH2-RH1}} = (\mathrm{GF_{VOL}} - 1)V_{\mathrm{RH1}}, \qquad [5]$$

where the upper limit for integration of aerosol volume is 2.5 μm for the ambient channel (D_{RH2}) and the upper limit for integration of the dried distribution is given by Equation (2). If we further assume minimal residual water content at the dried RH, then $\mathrm{V_{H2O,RH2-RH1}}$ is equal to $\mathrm{V_{H2O,RH2}}$, or the amount of aerosol water at ambient RH. Aerosol water contents for 1 July to 7 July 2001 calculated using this method are shown by the filled squares in Figure 9b and as a fraction of total dried aerosol mass in Figure 9d. These time series correspond to ambient channel RHs shown in Figure 9a. Figure 9 shows that the DAASS system has good dynamic range in the aerosol water content measurements, ranging from less than 1 μg/m^3 of water up to 20–30 μg/m^3 of water and from less than 5% of the dried aerosol mass to around 100% of the dried aerosol mass. Furthermore, the time response is excellent, with experimental system and data reduction methods following rapid changes in aerosol volume, aerosol water content, and hygroscopicity.

Calculation of Efflorescence Branch Humidigrams. Aerosol water content is a function of RH, chemical composition, and state of hydration (deliques cence branch or efflorescence branch). When aerosol water content is a smooth function of RH (e.g., moving on the efflorescence branch without crystallization) growth factors as a function of RH can be fit to simple empirical functions. For significant periods of the PAQS, growth factors were a smooth function of RH, with no apparent deliquescence or crystallization behavior (Khlystov et al. 2004b). Therefore, groups of growth factors representing relatively constant aerosol composition but with different RHs could be fit to an empirical function such as that used by Dick et al.

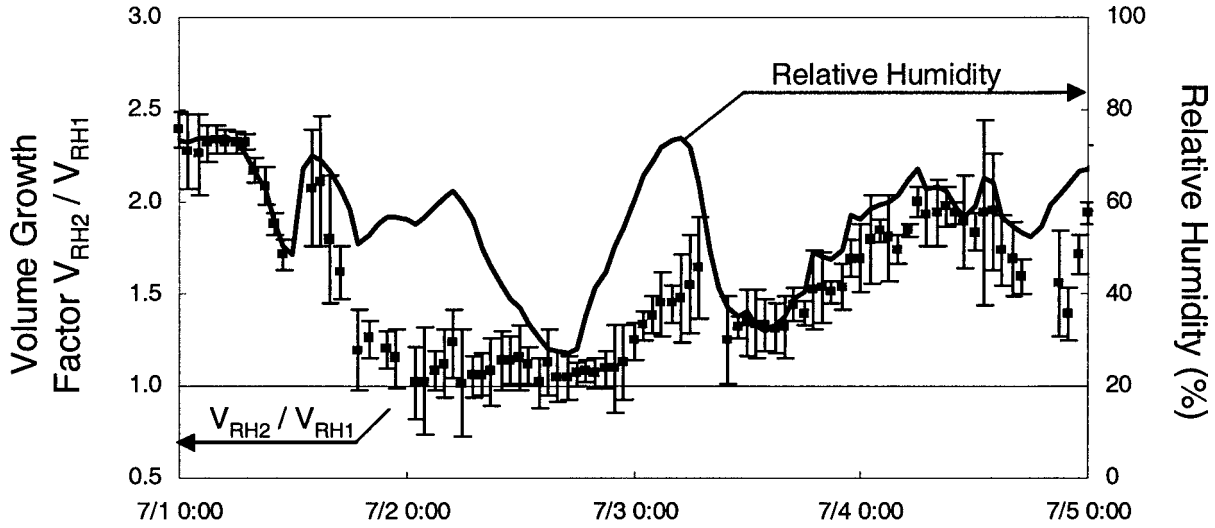

Figure 8. Sample results of volume growth factors as measured by the DAASS for 1 July to 4 July 2001. The RH trace is the RH of the ambient channel. The RH of the dried samples was 18 ± 6%.

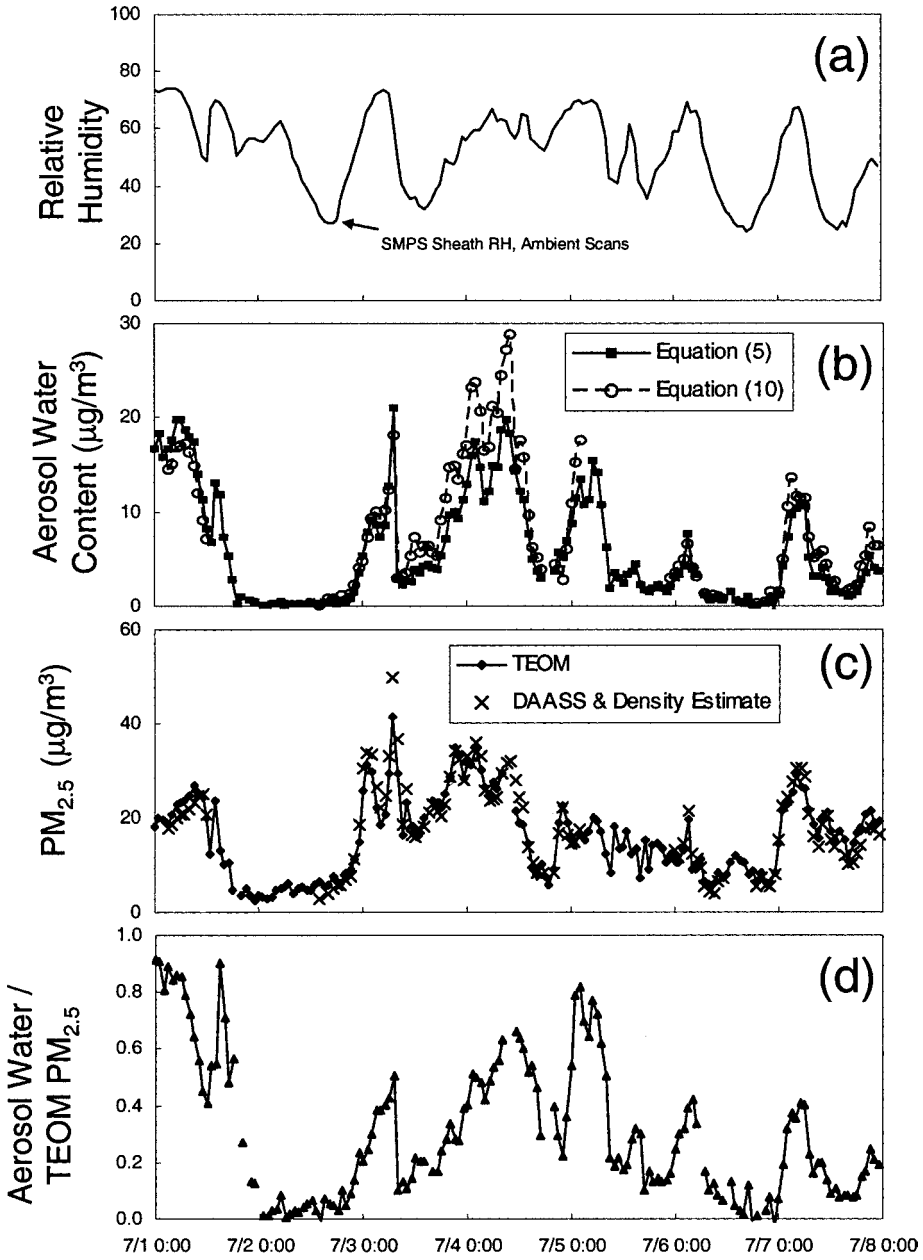

Figure 9. Example of aerosol water content measurement for a 7-day period. (a) ambient channel RH; (b) calculated mass of aerosol water by the difference of ambient and dried volume (Equation (5)) and using an estimated mass growth factor (Equation (10)); (c) $PM_{2.5}$ measured by TEOM (circles and solid line) and using the DAASS measured volume and composition-based density estimate ($\times$ symbols); and (d) ratio of measured water to the TEOM. As noted in the experimental section, these samples are from the time period when the DMA columns were inside the enclosure, and the outdoor RH may be up to 20% higher than the ambient channel value in the figure.

(2000):

$$\frac{V(\mathrm{RH})}{V_{\mathrm{dry}}} = 1 + (a + b\mathrm{RH} + c\mathrm{RH}^2)\frac{\mathrm{RH}}{1 - \mathrm{RH}}, \qquad [6]$$

where a, b, and c are adjustable parameters. In conjunction with DAASS-determined volume growth factors $\mathrm{GF_{VOL}}$, the parameters a, b, and c could be determined by regression:

$$\mathrm{GF_{VOL}} = \frac{1 + \left(a + b\mathrm{RH2} + c\mathrm{RH2}^2\right)\frac{\mathrm{RH2}}{1-\mathrm{RH2}}}{1 + \left(a + b\mathrm{RH1} + c\mathrm{RH1}^2\right)\frac{\mathrm{RH1}}{1-\mathrm{RH1}}}. \qquad [7]$$

Examples of the humidigrams calculated using groups of measured growth factors are shown in Figure 10. The difference in

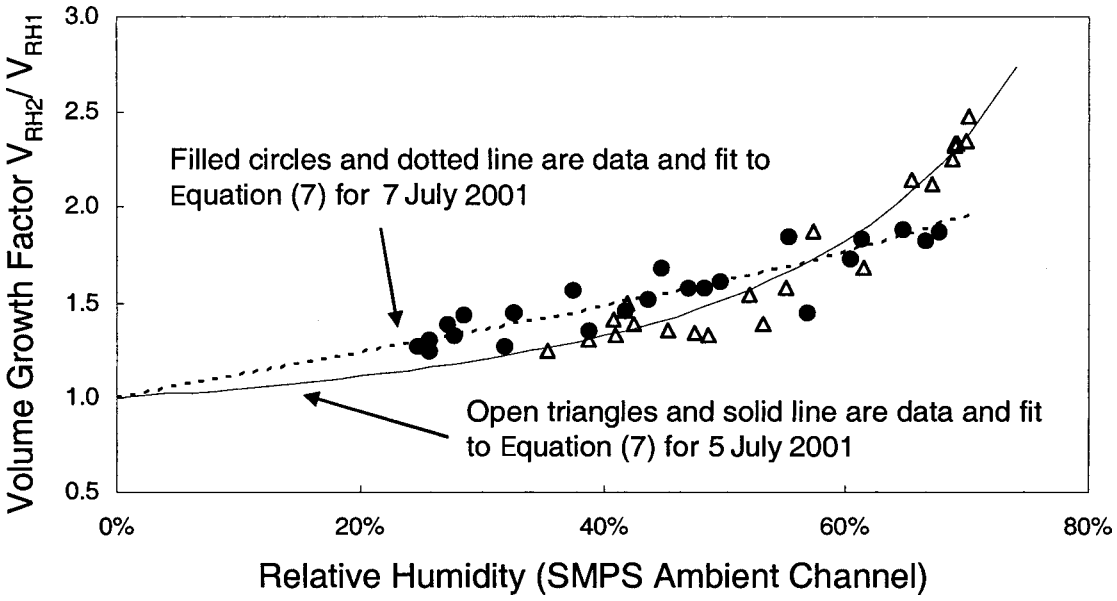

Figure 10. Example of humidigrams for two different days (5 and 7 July 2001). Points are measured hourly volume growth factors, and lines are fits of the hourly data to Equation (7).

the humidigrams between these two time periods is probably related to the aerosol chemistry, which contained more organic matter (52 wt%) on 7 July than on 5 July (38 wt%).

In certain applications, it is necessary to calculate aerosol water content at a specific RH. For example, DAASS data has been used to help estimate residual aerosol water in filter-based samples equilibrated at RHs from 15–35% (Rees et al. 2003). The calculation of residual water is performed using Equation (6), subject to the assumptions discussed above.

Calculation of the Mass Growth Factor. For comparison of volume growth factors to models and correlations involving mass growth factors, it can be useful to convert the DAASS-measured volume growth factors to mass growth factors. To do this we need to estimate the density of the aerosols as a function of RH using aerosol composition information from sources other than the DAASS instrument. The equations involved in the conversion from the volume to mass growth factor, and a simple method for density estimation during the PAQS, are developed below.

The volume and mass growth factors are related by Equation (8),

$$\mathrm{GF_{MASS}} = \mathrm{GF_{VOL}}\frac{\rho_{\mathrm{RH2}}}{\rho_{\mathrm{RH1}}}, \qquad [8]$$

where ρ_{RH2} and ρ_{RH1} are the hydrated (RH2) and dried (RH1) densities.

With this mass-based growth factor in hand, a mass-based estimate of aerosol water content can be made and compared to the volume-based calculation in Equation (5). The remainder of this section first covers the aerosol water mass balance, and then methods for aerosol density estimation for the PAQS are developed.

This definition of the mass growth factor can be used to write the aerosol mass balance (assuming water is the only semivolatile species that partitions as RH changes). If $\mathrm{M_{dry}}$ is the completely dehydrated aerosol mass, $\mathrm{M_{H2O,RH2\text{-}RH1}}$ is the water released from the aerosol as it dries from ambient RH ($\mathrm{RH_2}$) to the dried channel RH (RH1), and $\mathrm{M_{H2O,RH1}}$ is the residual aerosol water at the dried RH (RH1), then

$$\begin{aligned} M_{\mathrm{RH2}} &= M_{\mathrm{dry}} + M_{\mathrm{H2O,RH2-RH1}} + M_{\mathrm{H2O,RH1}} \\ &= (M_{\mathrm{dry}} + M_{\mathrm{H2O,RH1}})\mathrm{GF_{MASS}}, \end{aligned} \qquad [9]$$

where ρ_{RH2} and ρ_{RH1} are the hydrated (RH2) and dried (RH1) densities. $M_{\mathrm{H2O,RH2-RH1}}$ is the water released from the aerosol as it dries from ambient RH (RH2) to the dried channel RH (RH1). Conceptually, there are three possibilities for the behavior of the aerosol water content as the aerosol is dehydrated. At the low RH all particles are dry, or they all have some water, or some of them lose water and some do not. The first case corresponds to $M_{\mathrm{H2O,RH1}}$ equal to zero. The other two cases correspond to nonzero values for $M_{\mathrm{H2O,RH1}}$. The DAASS instrument gives the measurement of $M_{\mathrm{H2O,RH2-RH1}}$. Since RH1 is kept as low as possible, $M_{\mathrm{H2O,RH1}}$ is expected to be small compared to $M_{\mathrm{H2O,RH2\text{-}RH1}}$. Assuming $M_{\mathrm{H2O,RH1}}$ is negligible, $M_{\mathrm{H2O,RH2}}$ is then given by Equation (10):

$$\begin{aligned} M_{\mathrm{H2O,RH2}} &\approx M_{\mathrm{dry}}(\mathrm{GF_{MASS}} - 1) \\ &= M_{\mathrm{dry}}\left(\mathrm{GF_{VOL}}\frac{\rho_{\mathrm{RH2}}}{\rho_{\mathrm{RH1}}} - 1\right). \end{aligned} \qquad [10]$$

The density calculations assume that the aerosol is an internal mixture consisting of inorganic matter, organic matter, and elemental carbon fractions, each with a fixed characteristic density. The dry density is calculated assuming volume additivity and that $M_{H2O,RH1}$ is negligible:

$$\rho_{RH1} = \left(\frac{f_{OM}}{\rho_{OM}} + \frac{f_{EC}}{\rho_{EC}} + \frac{f_{inorg,dry}}{\rho_{inorg,dry}} \right)^{-1}, \quad [11]$$

where f refers to mass fraction: ρ to density; and the subscripts OM, EC, and inorg, dry refer to organic matter, elemental carbon, and dry inorganic mass, respectively. The ambient humidity density is estimated assuming the aerosol consists of three fractions, a hydrated inorganic fraction, an elemental carbon fraction (assumed not to take up any water), and an organic fraction (assumed not to take up any aerosol water):

$$\rho_{RH2} = \left(\frac{f_{OM}}{\rho_{OM}} + \frac{f_{EC}}{\rho_{EC}} + \frac{f_{inorg,dry} + f_{H2O,RH2}}{\rho_{inorg,wet}} \right)^{-1}, \quad [12]$$

where $\rho_{inorg,wet}$ refers to the density of the hydrated inorganics.

For this work the $PM_{2.5}$ measured by a Tapered Element Oscillating Microbalance (TEOM, Rupprecht & Patashnick, Albany, NY) at 30°C with a sample equilibration system (Meyer et al. 2000) was used for M_{dry}. The mass measured by the instrument was in good agreement with the federal reference method for particulate mass during these tests (Rees et al. 2004). The sample equilibration system is a semipermeable membrane drying inlet for the TEOM that conditions the aerosol sample at 30°C and ~15% RH. The organic matter mass used for calculations in this study was 1.8 times the organic carbon (OC). Elemental carbon (EC) and OC were measured by the thermal optical method (Cabada et al. 2002). The 1.8 multiplier for carbonaceous mass is based on estimates of Turpin and Lim (2001). Densities of 1.2, 1.6, and 1.77 g/cm^{-3} were assumed for organic matter, elemental carbon aerosol, and dry inorganic aerosol, respectively. The organic matter density is based on Turpin and Lim (2001) and the dry inorganic mass corresponds to that of ammonium sulfate, the dominant inorganic component in the Pittsburgh area (Anderson et al. 2002). The elemental carbon density is most uncertain, as recent measurements show great variability in the effective density (0.2–1.6 g/cm^3) of soot agglomerates depending on formation conditions (Park et al. 2003 and references therein). However, because of the small contribution of EC to the total aerosol concentration in Pittsburgh, the specific value chosen has little effect on the volume to mass growth factor conversion in this study. The 1.6 g/cm^3 value used in this work is at the upper end of effective densities measured by Park et al. (2003) and at the lower end of the range for the physical density of graphite (Perry et al. 1984). The carbonaceous fraction is assumed to not take up any water in this work, and the hydrated density for ammonium sulfate, calculated using empirical values from Tang (1997), is used for the ambient RH inorganic density.

The main use of the Equations (8)–(12) is for comparison of experimental (volume-based) growth factors with mass-based growth factors from other sources (i.e., thermodynamic models). The comparison can be made on the basis of predicted versus measured aerosol water content or on the basis of predicted versus measured growth factors. In both cases, Equations (8)–(12) will be required to make the comparison. While this work does not contain any mass-based water content measurements or model predictions (see Khlystov et al. 2004b for model–measurement comparisons), this type of calculation is demonstrated by the open circles in Figure 9b, which are an estimate of aerosol water content from Equation (10) based on the DAASS-measured volume growth factors, estimates of aerosol density using Equations (11) and (12), and the time series of M_{dry} measured independently of the DAASS system. The difference between the water content calculation by Equations (5) and (10) can be attributed to (1) uncertainty in the density calculations, composition, and organic mass multiplier; (2) violations of assumptions such as nonhygroscopic organics and negligible water content in the dried channel; and (3) drifts in the absolute accuracies of the various independent instruments that are involved in making the volume-based aerosol calculations (SMPS & APS) and the mass-based calculations (TEOM, OC/EC sampler, and inorganic ions sampler). The mismatch is particularly evident during 3 and 4 July. In light of these possible errors and uncertainties, Equation (5) is recommended as a more robust estimate of aerosol water content than Equation (10). A further demonstration of the connection between aerosol mass, aerosol volume, and composition-based density estimates (all measured independently) is shown by the comparison in Figure 9c of M_{dry} measured by two independent techniques. The TEOM mass measurement is compared to the DAASS-estimated aerosol mass calculated using the density formula in Equation (11).

Discussion of Some Sources of Error

The following errors are discussed in this section: (1) charging of the aerosol at different RHs than classification; (2) potential for crystallization during water due to heated zones of inlet; and (3) differences in RH between the SMPS aerosol and sheath flows.

Differences in RH between the bipolar aerosol charger, aerosol flow entering the DMA, and DMA sheath flow can cause changes in the physical state of the particles and errors in particle sizing and/or counting. First, the aerosol may be charged in the bipolar charger while at a different RH (and therefore size) than in the DMA. Second, heated zones of the inlet prior to the classifier (which is at ambient temperature) may induce crystallization of the aerosol. Finally, the difference in the aerosol and sheath flows may cause a size change during size classification. The implications of these errors are discussed below.

Parts of the aerosol inlet (including the bipolar charger) were inside the enclosure, which was usually a few degrees warmer than the DMA column, located outside the enclosure. This caused the RH of the aerosol flow during ambient scans to go through a minimum inside the enclosure, at the time of aerosol charging. In winter, the enclosure (and bipolar charger) was

Table 1
Estimates in growth factor bias due to charging under dryer conditions than classification

Outside RH (%)	Outside temperature		
	5°C (%)	0°C (%)	(%) −5°C
50	+3	+3	+3
70	+2	+6	+6
85	+4	+6	+10
92	+7	+10	+14

maintained at 9°C, while outdoor temperatures dropped to approximately −5°C. As a result of these two effects, in general the aerosol charging was not at the same RH as the size classification in the DMA. For hydrated particles, this means that aerosols may be charged at one size and then classified at another, creating an error in the equilibrium charge distribution assumed during the inversion of the raw SMPS data. This generally leads to an underestimation in the particle number at sizes smaller than about 200 nm, and an overestimation at sizes greater than about 200 nm. The magnitude of this error was estimated using the study average size distribution and an assumed composition of 50% ammonium sulfate and 50% organics and other nonhygroscopic material. Volume growth factors are biased high by a factor of 1.00 to 1.14, with the greatest effects at low temperatures and humid conditions. Our error estimates are shown in Table 1.

The higher inlet temperatures compared to ambient caused temporary drying of the ambient channel aerosol before it was returned to ambient temperature for size classification. During the coldest periods of the study, this drying effect could be important. Therefore, the minimum RH experienced by the aerosol en route to classification is calculated and reported with the PAQS data to allow a more complete interpretation of the results.

Sheath-aerosol stream mismatch should not pose a problem as the thermodynamic equilibration time is expected to be short compared to the transit times in the DMAs (0.3 s and 6 s for the N-SMPS and SMPS, respectively). Characteristic times for equilibration of pure water droplets up to 1 micron in size under the conditions in the SMPS should be of order 10^{-3} s. There is evidence from laboratory studies that coatings of hydrophobic organics over salts (5–60 wt% organics) may hinder mass transfer (Wagner et al. 1996; Xiong et al. 1998), although the extension of these laboratory studies to atmospheric particles has not been established. To test the assumption that the sheath-aerosol RH mismatch did not significantly affect the results, an experiment was performed in 2002 during the PAQS where the SMPS aerosol was dried more thoroughly (∼20% RH) than usual (∼50% RH) while the sheath RH was held at around 5%. The organic fraction of the aerosol was between 30 and 50% on the day of the experiment, and the outdoor RH was between 85 and 95%. No shift in the dried aerosol size distribution could be detected due to the lower RH and increased time for mass transfer at low RH.

SUMMARY AND CONCLUSION

A system has been constructed for the in situ measurement of aerosol water content at atmospheric conditions. The system relies on a combination of aerosol sizing instruments and samples the atmospheric aerosol at ambient temperature and at two RHs. The DAASS measures the aerosol volume growth factor (ratio of the ambient and dried aerosol volume concentrations) and aerosol water content every 15 min. A variety of data reduction procedures were presented to convert the raw data to growth factors and aerosol water content, and (when combined with aerosol composition measurements) to facilitate comparison with mass-based growth factors from other sources. DAASS operated for a year during the PAQS.

The system was tested with ammonium sulfate particles equilibrated at different RHs, and its results were in good agreement with the known hygroscopic properties of the particles. The preliminary field results show good response to RH and dry particle mass with the water concentration varying from almost zero to more than 20 $\mu g/m^3$ (0–50% of the hydrated particle mass). The detailed measurements of water during PAQS and the comparison of these measurements with predictions of theoretical models are discussed in detail in a companion article (Khlystov et al. 2004b).

REFERENCES

Anderson, R. R., Martello, D. V., Rohar, P. C., Stazisar, B. R., Tamilia, J. P., Waldner, K., and White, C. M. (2002). Sources and Composition of $PM_{2.5}$ at the National Energy Technology Laboratory in Pittsburgh During July and August 2000, *Energy Fuels* 16:261–269.

Ansari, A. S., and Pandis, S. N. (1999). Prediction of Multicomponent Inorganic Atmospheric Aerosol Behavior, *Atmos. Environ.* 33:745–757.

Ansari, A. S., and Pandis, S. N. (2000). Water Absorption by Secondary Organic Aerosol and Its Effect on Inorganic Aerosol Behavior, *Environ. Sci. Technol.* 34:71–77.

Armendariz, A. J., and Leith, D. (2002). Concentration Measurement and Counting Efficiency for the Aerosol Particle Sizer 3320, *J. Aerosol Sci.* 33:133–148.

Berg, O. H., Swietlick, E., and Krejci, R. (1998). Hygroscopic Growth of Aerosol Particles in the Marine Boundary Layer Over the Pacific and Southern Oceans During the First Aerosol Characterization Experiment, *J. Geophys. Res.* 103(D13):16,535–16,545.

Brooks, S., Wise, M., Cushing, M., and Tolbert, M. (2002). Deliquescence Behavior of Organic/Ammonium Sulfate Aerosol, *Geophys. Res. Lett.* 29:1917, DOI: 10.1029/2002GL014733.

Cabada, J. C., Pandis, S. N., and Robinson, A. L. (2002). Sources of Atmospheric Carbonaceous Particulate Matter in Pittsburgh, Pennsylvania, *J. Air Waste Manage.* 52(6):732–741.

Chan, C. K., Flagan, R. C., and Seinfeld, J. H. (1992). Water Activities of Ammonium Nitrate/Ammonium Sulfate Solutions, *Atmos. Environ.* 26A(9):1661–1673.

Clegg, S. L., Seinfeld, J. H., and Brimblecombe, P. (2001). Thermodynamic Modeling of Aqueous Aerosols Containing Electrolytes and Dissolved Organic Compounds, *J. Aerosol Sci.* 32(6):713–738.

Cocker, D. R., III, Clegg, S. L., Flagan, R. C., and Seinfeld, J. H. (2001a). The Effect of Water on Gas-Particle Partitioning of Secondary Organic Aerosol. Part I: α-Pinene/Ozone System, *Atmos. Environ.* 35:6049–6072.

Cocker, D. R., III, Mader, B. T., Kalberer, M., Flagan, R. C., and Seinfeld, J. H. (2001b). The Effect of Water on Gas-Particle Partitioning of Secondary Organic Aerosol: II. m-Xylene and 1,3,5-Trimethylbenzene Photooxidation Systems, *Atmos. Environ.* 35:6073–6085.

Cocker, D. R., III, Whitlock, N. E., Flagan, R. C., and Seinfeld, J. H. (2001c). Hygroscopic Properties of Pasadena, California Aerosol, *Aerosol Sci. Technol.* 35:637–647.

Cruz, C. N., and Pandis, S. N. (2000). Deliquescence and Hygroscopic Growth of Mixed Inorganic-Organic Atmospheric Aerosol, *Environ. Sci. Technol.* 34:4313–4319.

Day, D. E., Malm, W. C., and Kreidenweis, S. M. (2000). Aerosol Light Scattering Measurements as a Function of Relative Humidity, *J. Air Waste Manage.* 50:710–716.

Dick, W. D., Saxena, P., and McMurry, P. H. (2000). Estimation of Water Uptake by Organic Compounds in Submicron Aerosols Measured During the Southeastern Aerosol and Visibility Study, *J. Geophys. Res.* 105(D1):1471–1479.

Han, J., and Martin, S. T. (1999). Heterogeneous Nucleation of the Efflorescence of $(NH_4)_2SO_4$ Particles Internally Mixed with Al_2O_3, TiO_2, and ZrO_2, *J. Geophys. Res.* 104:3543–3554.

Han, J.-H., Hung, H.-M., and Martin, S. T. (2002). Size Effect of Hematite and Corundum Inclusions on the Efflorescence Relative Humidities of Aqueous Ammonium Nitrate Particles, *J. Geophys. Res.* 107, DOI: 10.1029/2001JD001054.

Hanel, G. (1976). The Properties of Atmospheric Aerosol Particles as Functions of Relative Humidity at Thermodynamic Equilibrium with Surrounding Moist Air. In *Advances in Geophysics, Vol. 19*, H. E. Landsberg and J. Van Mieghem, eds., Academic Press, New York, pp. 73–188.

Khlystov, A., Stanier, C., and Pandis, S. N. (2004a). An Algorithm for Combining Electrical Mobility and Aerodynamic Size Distribution Data when Measuring Ambient Aerosol, *Aerosol Sci. Technol.* 38:229–238.

Khlystov, A., Stanier, C., Takahama, S., and Pandis, S. N. (2004b). Water Content of Ambient Aerosols During the Pittsburgh Air Quality Study, *J. Geophys. Res.* Submitted.

Kreisberg, N. M., Stolzenburg, M. R., and Hering, S. V. (2001). A New Method for Measuring the Dependence of Particle Size Distributions on Relative Humidity, with Application to the Southeastern Aerosol and Visibility Study, *J. Geophys. Res.* 106:14,935–14,949.

Lee, C. T., and Hsu, W. C. (1998). A Novel Method to Measure Aerosol Water Mass, *J. Aerosol Sci.* 29(7):827–837.

Leinert, S., and Wiedensohler, A. (2000). APS Counting Efficiency Calibration for Submicrometer Particles, *J. Aerosol Sci.* 31:S404–S405.

Martin, S. T., Han, J., and Hung, H. M. (2001). The Size Effect of Hematite and Corundum Inclusions on the Efflorescence Relative Humidities of Aqueous Ammonium Sulfate Particles, *Geophys. Res. Lett.* 28:2601–2604.

Meyer, M. B., Patashnick, H., Ambs, J. L., and Repprecht, E. (2000). Development of a Sample Equilibration System for the TEOM Continuous PM Monitor, *J. Air Waste Manage.* 50(8):1345–1349.

McMurry, P. H., and Stolzenberg, M. (1989). On the Sensitivity of Particle Size to Relative Humidity for Los Angeles Aerosols, *Atmos. Environ.* 23(2):497–507.

Ming, Y., and Russell, L. M. (2002). Thermodynamic Equilibrium of Organic-Electrolyte Mixtures in Aerosol Particles, *AICHE Journal* 48:1331–1348.

Ohta, S., Hori, M., Yamagata, S., and Murao, N. (1998). Chemical Characterization of Atmospheric Fine Particles in Sapporo with Determination of Water Content, *Atmos. Environ.* 32(6):1021–1025.

Onasch, T. B., Siefert, R. L., Brooks, S. D., Prenni, A. J., Murray, B., Wilson, M. A., and Tolbert, M. A. (1999). Infrared Spectroscopic Study of the Deliquescence and Efflorescence of Ammonium Sulfate Aerosol as a Function of Temperature, *J. of Geophys. Res.* 104(D17): 21,317–21,326.

Park, K., Cao, F., Kittelson, D., and McMurry, P. H. (2003). Relationship Between Particle Mass and Mobility for Diesel Exhaust, *Environ. Sci. Technol.* 37:577–583.

Peng, C., Chan, M. N., and Chan, C. K. (2001). The Hygroscopic Properties of Dicarboxylic and Multifunctional Acids: Measurements and UNIFAC Predictions, *Environ. Sci. Technol.* 35(22):4495–4501.

Perry, R. H., Green, D. W., and Maloney, J. O. (1984). *Perry's Chemical Engineering Handbook*, 6th ed., McGraw Hill: New York, pp. 3–96.

Rader, D. J., and McMurry, P. H. (1986). Application of the Tandem Differential Mobility Analyzer to Studies of Droplet Growth or Evaporation, *J. Aerosol Sci.* 17(5):771–787.

Rees, S. L., Robinson A. L., Khlystov, A., Stanier, C. O., Pandis, S. N. (2004). Mass Balance Closure and the Federal Reference Method for $PM_{2.5}$ in Pittsburgh, Pennsylvania, *Atmos. Environ.* in press.

Rood, M. J., Covert, D. S., and Larson, T. V. (1987). Temperature and Humidity Controlled Nephelometry: Improvements and Calibration, *Aerosol Sci. Technol.* 7:57–65.

Saxena, P., and Hildemann, L. M. (1997). Water Absorption by Organics: Survey of Laboratory Evidence and Evaluation of UNIFAC for Estimating Water Activity, *Environ. Sci. Technol.* 31:3318–3324.

Speer, R. E., Barnes, H. M., and Brown, R. (1997). An Instrument for Measuring the Liquid Water Content of Aerosols, *Aerosol Sci. Technol.* 27(1): 50–61.

Tang, I. N., and Munkelwitz, H. R. (1993). Composition and Temperature Dependence of the Deliquescence Properties of Hygroscopic Aerosols, *Atmos. Environ.* 27A:467–473.

Tang, I. N. (1997). Thermodynamic and Optical Properties of Mixed-Salt Aerosols of Atmospheric Importance, *J. Geophys. Res.* 102:1883–1893.

ten Brink, H. M., Khlystov, A., Kos, G. P. A., Tuch, T., Roth, C., and Kreyling, W. (2000). High-Flow Humidograph for Testing the Water Uptake by Ambient Aerosol, *Atmos. Environ.* 34:4291–4300.

Turpin, B., and Lim, H. (2001). Species Contributions to $PM_{2.5}$ Mass Concentrations: Revisiting Common Assumptions for Estimating Organic Mass, *Aerosol Sci. Technol.* 35:602–610.

Vartiainen, M., McDow, S. R., and Kamens, R. M. (1994). Water Uptake by Aerosol Particles from Automobile Exhaust and Wood Smoke, *Chemosphere* 29:1661–1669.

Virkkula, A., Van Dingenen, R., Raes, F., and Hjorth, J. (1999). Hygroscopic Properties of Aerosol Formed by Oxidation of Limonene, α-Pinene, and β-Pinene, *J. Geophys. Res.* 104(D3):3569–3579.

Wagner, J., Andrews, E., and Larson, S. M. (1996). Sorption of Vapor Phase Octanoic Acid Onto Deliquescent Salt Particles, *J. Geophys. Res.* 101(D14):19,533–19,540.

Willeke, K., and Baron, P. A. (1993). *Aerosol Measurement Principles, Techniques, and Applications.* Van Nostrand Reinhold: New York.

Woo, K. S., Shi, Q., Sakurai, H., and McMurry, P. H. (2001). A Relative Humidity Conditioner for Atmospheric Sampling. *Presented at the American Association of Aerosol Research.* Portland, Oregon, October 2001.

Xiong, J. Q., Zhong, C. F., Chen, L. C., and Lippmann, M. (1998). Influence of Organic Films on the Hygroscopicity of Ultrafine Sulfuric Acid Aerosol, *Environ. Sci. Technol.* 32:3536–3541.

Yi, M., and Russell, L. M. (2002). Thermodynamic Equilibrium of Organic-Electrolyte Mixtures in Aerosol Particles. *AIChE J.* 48(6):1331–1348.